N72-22046

Tyco Laboratories, Inc.
Bear Hill
Waltham, Massachusetts 02154

NiCd BATTERY ELECTRODES

C - 150

First Quarterly Report

by

G. Holleck

Contract No. 953185-NAS7-100

November 1971

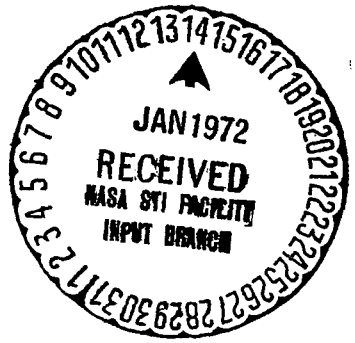

This work was performed for the Jet Propulsion Laboratory, California Institute of Technology sponsored by the National Aeronautics and Space Administration under Contract NAS7-1000.

NiCd BATTERY ELECTRODES
C - 150

First Quarterly Report

by

G. Holleck

Contract No. 953185-NAS7-100

November 1971

This work was performed for the Jet Propulsion Laboratory, California Institute of Technology sponsored by the National Aeronautics and Space Administration under Contract NAS7-1000.

ABSTRACT

The objective of this research program is to develop and evaluate electrodes for a nongassing negative limited nickel-cadmium cell. The concept of the negative limited cell and its implications on electrode structure are discussed. The key element is the development of a cadmium electrode with high hydrogen overvoltage. For this, Teflon-bonded Cd electrodes and silver-sinter based Cd electrodes were manufactured and in preliminary experiments their physical and electrochemical characteristics were evaluated. Hydrogen evolution on cadmium was found to occur approximately 100 mV more cathodic than on silver. Both electrode structures exhibit a fairly sharp potential rise at the end of the charging cycle and the advent of gas evolution occurs at potentials between -1.2 and -1.3 V versus a Hg/HgO reference electrode. These results are compared with conventional Ni-sinter based Cd electrodes.

Table of Contents

		Page No.
	ABSTRACT	ii
I.	THE NON-GASSING NiCd CELL, BACKGROUND AND APPRAISAL	1
II.	EXPERIMENTAL PROGRAM	4
	A. Hydrogen Overvoltage Studies	4
	B. Electrochemical Test Cell Design	4
	C. Development of Negative Electrode Structures	9
III.	FUTURE WORK	26
IV.	REFERENCES	27

List of Illustrations

Figure No.		Page No.
1.	H_2 Evolution on Ag and Cd in 25% KOH.	5
2.	Three Part Plexiglass Cell	6
3.	Electrochemical Test Cell (disassembled)	7
4.	*Electrochemical Test Cell (assembled)*	8
5.	Charge and Discharge Cycles of Teflon-bonded Cd Electrode TFE-1	11
6.	Charge and Discharge Cycles of Teflon-bonded Cd Electrode TFE-2	12
7.	Charge and Discharge Cycles of Teflon-bonded Cd Electrode TFE-3	13
8.	Ag Sinter Plaque (Silpowder 150, FAPD 10.4 μ, dry layup).	17
9.	Ag Sinter Plaque (Silpowder 150, FAPD 15.2 μ, dry layup).	18
10.	Ag Sinter Plaque (Silpowder 220, NaF compact)	19
11.	Ni Plaque.	20
12.	Ag Sinter Cd Electrode, SSCd-1.	22
13.	Ag Sinter Cd Electrode, SSCd-1.	23

I. THE NON-GASSING NiCd CELL, BACKGROUND AND APPRAISAL

In the following we summarize the known characteristics of the positive and negative plates in present NiCd batteries. This will allow us to define the constraints in both plate manufacture and cell operation that are relevant to the implementation of the present program.

The present design of hermetically sealed cells depends on:

1. Preventing H_2 evolution at the negative on charge by providing a large excess negative plate capacity.

2. Limiting oxygen evolution at the positive plate to a rate at which oxygen can be recombined at the negative plate.

In concept, this mode of operation is sound; in practice, the capacity of the negative plate decays, eventually leading to H_2 generation and cell failure. (There is no effective mechanism for H_2 recombination in NiCd cells.) In effect, these statements define the principal characteristics of nickel-cadmium battery plates that must be accommodated in a sealed cell design: (1) the inherent inefficiency of charge acceptance at the positive plate, and (2) the requirement to avoid H_2 evolution at the negative plate. Initially, let us examine these two problems in the context of the proposed configuration of the nongassing cell. The gassing reactions on cell reversal in a bettery and the particular problems associated with operation at temperature extremes will be considered later.

The principal design modification proposed for the nongassing NiCd cell is that the ratio of the negative to positive capacities be such that the negative plate, rather than the positive plate, is limiting. Under these circumstances, overcharge cannot be tolerated and it is necessary to clearly identify the fully charged condition without an appreciable time lag. This is most easily realized in practice by eliminating low overvoltage materials from the negative plate. The onset of hydrogen

evolution is then marked by a sharp increase in cell voltage, i.e., a signal that can be used to terminate the charging process.

Again, as with the positive limited cell, the system is sound in concept. Any oxygen generated due to inefficient charge acceptance by the positive active material can still be consumed at the negative plate, thus maintaining the initial capacity ratio. This is one of the principal advantages of the negative limited cell. The capacity of the cell positive plate, since overcharge is avoided, will slavishly follow the available capacity of the negative plate. Thus, any fade in negative capacity will be manifested only as a loss in cell capacity and will not result in catastrophic pressure buildup as occurs with the conventional positive limited cell. If negative fade is a reversible process, a series of conditioning cycles may restore the negative plate capacity, then the positive plate will still be able to match the improved negative capacity.

There are good arguments for the use of positive plates with appreciable excess capacity in negative limited batteries. For example, if excess capacity in the charged state (precharge) is built into the positive plate, the cell can tolerate limited cell reversal if it is capable of withstanding some internal pressure. Oxygen recombination is then averaged out over the whole duty cycle. More specifically, positive precharge permits oxygen accumulation in the cell without the cell becoming positive limited. This could give more flexible operation if occasional arduous duty cycles are involved.

There is also a good argument for excess positive capacity in the discharged state to such an extent that the plate can cycle below 70% of its rated capacity. Below the 70% of state of charge, charge acceptance is almost 100% efficient at normal charging rates and temperatures[1] and the self-discharge rates are lower.*

The proposed design in which the total capacity of the positive would be twice that of the negative does not lead to an excessive penalty in energy density when compared to conventional cells. By reducing the quantity of cadmium necessary for a particular nominal capacity, one compensates for the excess positive material required. Cell volume and configuration need not be compromised either, since

---

*In the absence of overcharge, very little of the γ form of the charged active material will be produced.[2] The γ "NiOOH"[3] in which the nickel valence is greater than three is considered to have a much higher self-discharge rate than the tervalent β-NiOOH.

positive plates of high specific capacity (8-10 Ahr/in.^{3}) can be prepared by electrochemical impregnation methods.[4,5] The experience with Ni-Cd batteries seems to indicate that a more lightly loaded negative plate shows better utilization and longer life.

There are further aspects of sealed cell operation that require further investigation. One of these is the fading of cadmium negative electrodes. Very little is known about the fading mechanism; however, there might be a correlation with the extent of O_2 recombination which would be much smaller than in conventional designs. This would also avoid the problem of heat generation towards the end of the charging cycle.

Another factor worthy of consideration is the effect cell operation with flooded electrolyte might have on the loss of capacity in the negative plate. It has been suggested that concentration gradients are responsible for cadmium migration.[6] In the flooded condition, the magnitude of these gradients may be different.

The negative limited cell also offers advantages in the event of limited accidental cell reversal. H_2 evolution would be avoided as long as part of the excess positive capacity is present in the charged state at the time of sealing. (It is envisioned that the cell would normally cycle between 20% and 70% state of charge.) Thus, on cell reversal, O_2 would be evolved at the negative plate and hydrogen would not be generated until the excess positive capacity in the positive was discharged. Oxygen evolution on the negative plate could also be avoided by inclusion of an antipolar mass to ensure gas free operation on limited cell reversal.

II. EXPERIMENTAL PROGRAM

A. Hydrogen Overvoltage Studies

Exploratory measurements of the overvoltage for hydrogen evolution at a silver wire (0.78 cm^2) and a flattened cadmium bead (six 9's Cd, 0.55 cm^2) have been carried out. Tafel plots (log I versus E) at these two electrodes are shown in Fig. 1. At current densities above 0.1 mA/cm^2, hydrogen evolution on cadmium occurs approximately 100 mV more cathodic than on silver. At lower current densities, cadmium apparently exhibits a lower hydrogen overvoltage than the silver. This result may be due to reducible impurities (smooth electrodes are very sensitive to impurity effects) or to slow reduction of intergranular cadmium oxide. Neither of these effects would influence the current-voltage characteristics of a high surface area porous electrode. Comparison of the hydrogen overvoltage characteristics of silver and cadmium should be deferred until we have made measurements on porous electrodes. It should be mentioned here that Lee[7] reported measurements of the hydrogen overpotential on cadmium electrodes in 6N KOH which agreed very well with our data above a current density of 0.1 mA/cm^2. However, Lee's investigation did not extend to lower current densities.

B. Electrochemical Test Cell Design

The three-compartment cell for the electrochemical evaluation is schematically shown in Fig. 2. Figs. 3 and 4 show the test cell arrangement before and after assembly. The cell consists of three plexiglass parts with silicone rubber gaskets and allows for two symetrically located counterelectrodes (positive plates) and a mercuric oxide reference electrode as well as gas inlets for electrolyte gas presaturation. The transparent cell permits visual observation of the electrode surface and quantitative measurement of the gas evolved via microburette. The cell is sealed from the atmosphere by specially molded silicone rubber stoppers. Temperature will be controlled by immersion in a thermostatted bath.

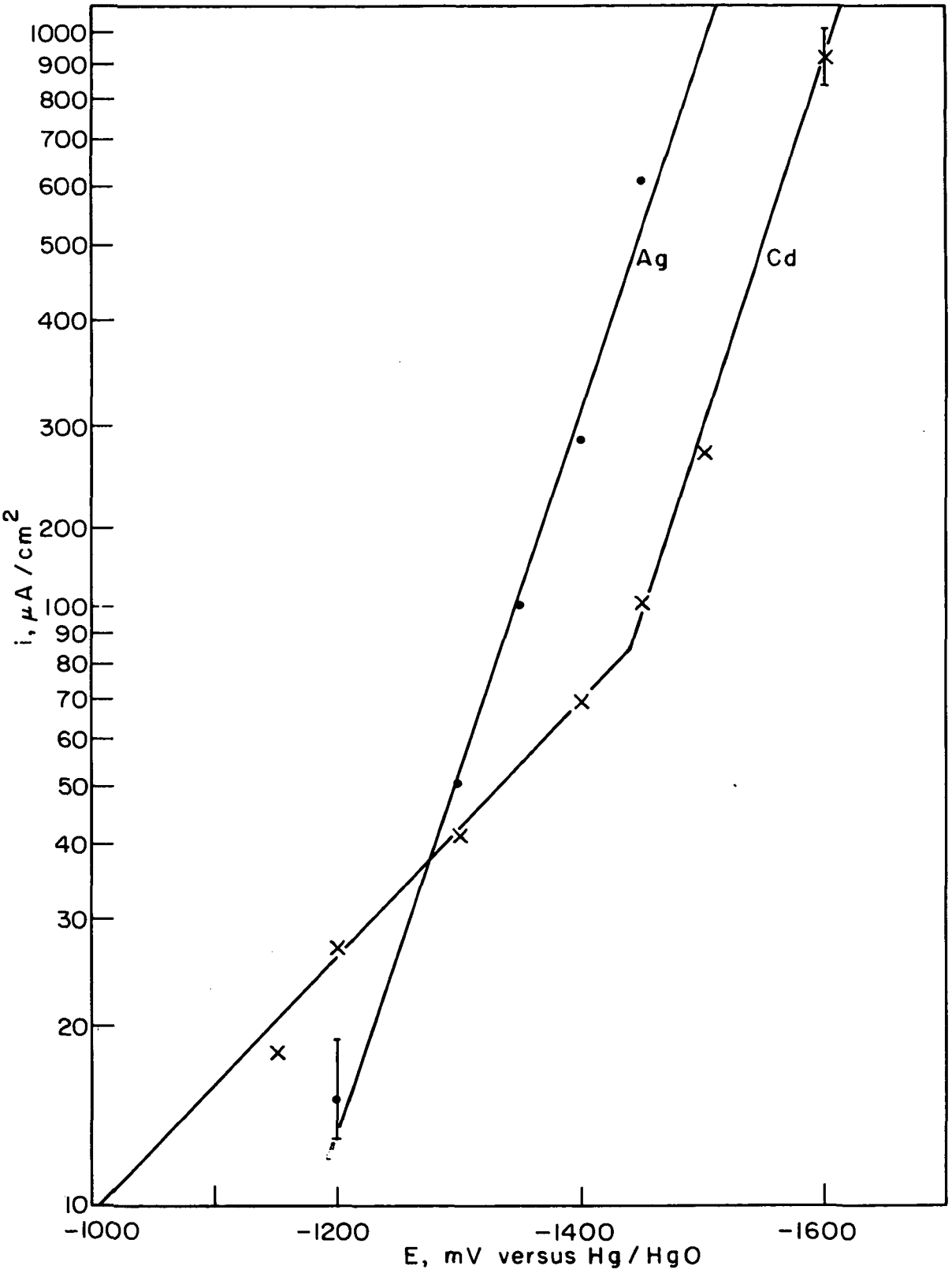

Fig. 1. H_2 evolution on Ag and Cd in 25% KOH (room temperature)

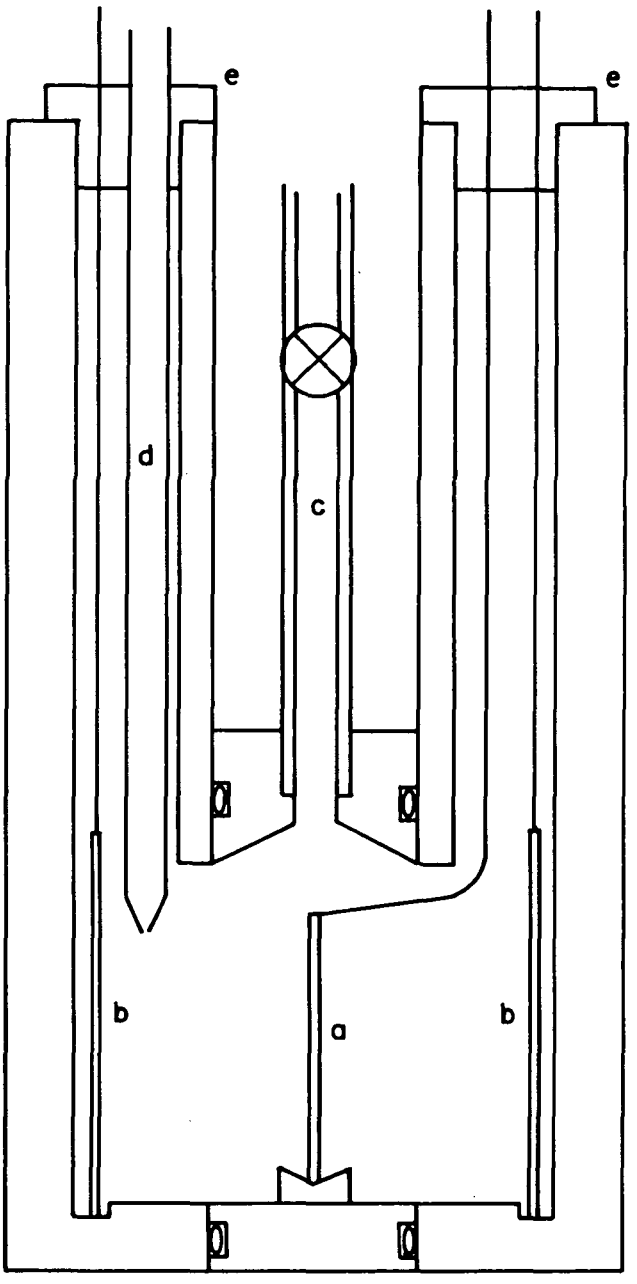

Fig. 2. Three part plexiglass cell [(a) negative plate, (b) positive plate, (c) calibrated gas burette, (d) Hg/HgO reference electrode, (e) silicone rubber seal]

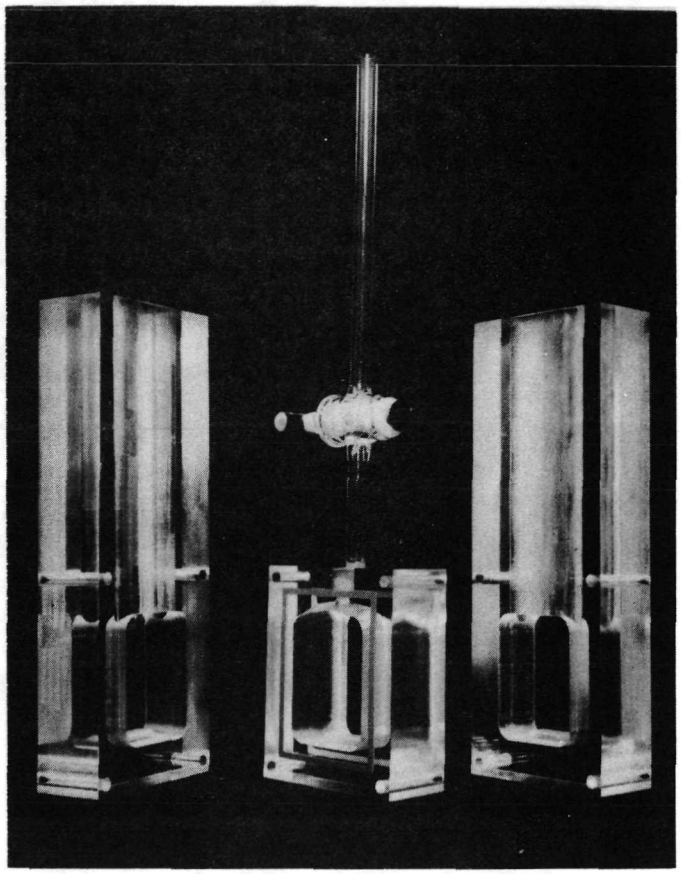

Fig. 3. Electrochemical test cell (disassembled)

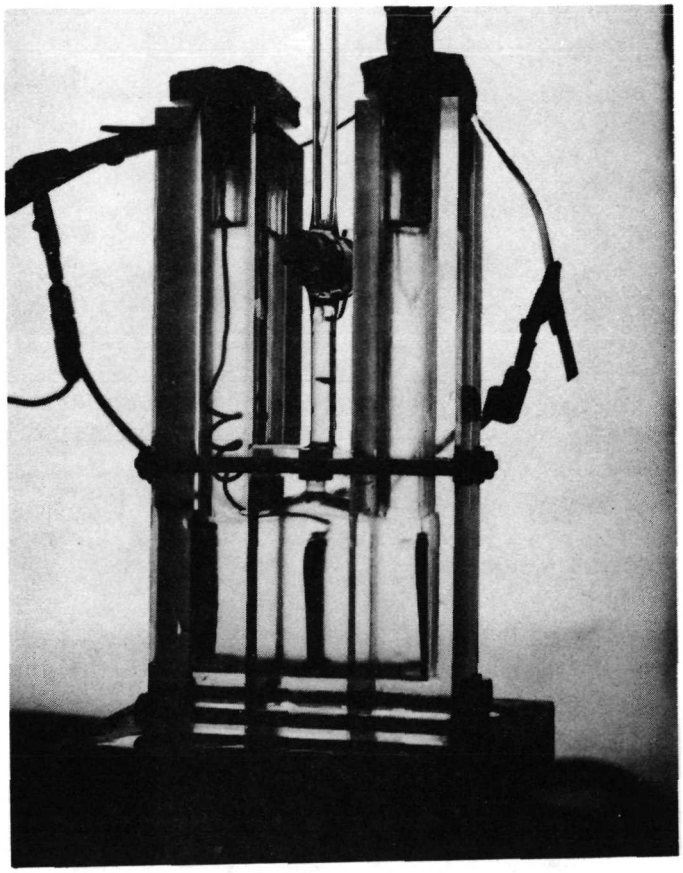

Fig. 4. Electrochemical test cell (assembled)

C. Development of Negative Electrode Structures

The objective of this phase of the program is to perform a feasibility study of negative plate fabrication techniques and examine the electrochemical behavior of the various structures proposed for negative plates. The structures which have been proposed include:

1. Silver sinter on silver screen
2. Teflon-bonded cadmium hydroxide on silver screen
3. Cadmium sinter on silver screen
4. Cadmium sinter on cadmium screen
5. Teflon-bonded cadmium hydroxide on cadmium screen
6. Electrodeposited porous cadmium sponge on silver or cadmium screen

In all cases, the starting materials must be carefully defined, especially with respect to particle size and particle size distribution. The structures obtained will be characterized including measurement of porosity, pore size and physical properties. Their electrochemical behavior will then be studied on plates 1 × 1.5 in.

In the second phase of this program, we will examine the appropriate structural variables (e.g., porosity, pore size distribution, thickness, loading, etc.) in order to obtain optimum electrode performance and conduct a detailed electrochemical testing program.

1. Teflon-bonded cadmium electrodes

a. Preparation: Cadmium hydroxide was prepared by rapid addition of 8.5N KOH (4% in excess of the stoichiometric amount) to a vigorously stirred 0.3M $Cd(NO_3)_2$ (Baker Reagent Grade) solution at 70 °C. The white precipitate was filtered, washed with triply distilled water to neutrality, and dried at 65 °C.

Teflon-bonded cadmium electrode TFE-1 was prepared by pasting a mixture of $Cd(OH)_2$, 5% Ag powder (Handy and Harman, Silpowder 150), 4.2% Teflon (DuPont Teflon 30) and sufficient water to obtain a thick paste onto a silver screen (Exmet 5 Ag 10 3/0). The electrode was then dried at 70 °C in air and vacuum followed by sintering at 275 °C for 20 min in an argon atmosphere. The resulting structure had a brown appearance due to the conversion of $Cd(OH)_2$ to CdO and showed small cracks from shrinking. The electrode was pressed at 0.7 ton/in.^{2} for 15 sec prior to testing.

Electrode TFE-2 was prepared by drying and sintering a mixture of $Cd(OH)_2$, Ag, and Teflon of the composition given above. The resulting brown, slightly tacky powder was pressed into an electrode at a pressure of 7 ton/in.^{2}. The substrate was expanded silver (5 Ag 7, 4/0).

Electrode TFE-3 contained 78.2% CdO, 8.7% Teflon and 12.1% silver flake. It was prepared by a combination of the above methods: Half of the wet mixture was distributed into a mold, the expanded silver screen (5 Ag 7, 4/0) placed on it, and the remaining paste was then added. After drying at 65 °C in vacuum, the structure was pressed at 7 tone/in.^{2} and sintered for 20 min at 180 °C in argon atmosphere.

b. Electrochemical evaluation of Teflon-bonded structures: All electrodes were tested in the electrochemical cell described above. They were subjected to a number of charge-discharge cycles between -1.2 V and -0.85 V versus Hg/HgO at current densities corresponding to rates between C and C/2. Occasionally the charging cycle was allowed to continue beyond the -1.2 V (versus Hg/HgO) cutoff voltage and the gassing behavior of the electrodes was observed. Representative charge and discharge curves for the three electrodes are shown in Figs. 5, 6, and 7. The basic shape of the potential-time curves is similar for all three electrodes. The potential is fairly constant during the charging process followed by a fairly rapid potential increase towards the end of the charging cycle. In some instances, the potential rise at the end of the charging cycle showed a plateau (Figs. 5 and 7) presumable reflecting the reduction of that $Cd(OH)_2$ which is not in good electronic contact with the screen.

Small individual gas bubbles at the electrode were initially observed at potentials above -1.2 V (versus Hg/HgO). At electrodes TFE-1 and -2, significant gas evolution did not occur until -1.3 to -1.4 V. At electrode TFE-3, which contained a larger amount of silver as a conductive filler (~12% versus 5%), the gassing occurred approximately 50 mV less negative. All electrodes continue to accept charge well beyond the beginning of gas evolution. Electrode TFE-1 showed some light shedding at the end of cycling while electrode TFE-2 exhibited considerable shedding. Electrode TFE-3 showed surface disruption but practically no shedding. The high and continuously increasing value of the charging potential (particularly with electrode TFE-2) as well as the additional charge acceptance beyond the start of gas evolution appear to be due to lack of good electronic contact between the current collector grid and active materials thus giving rise to an ohmic potential drop.

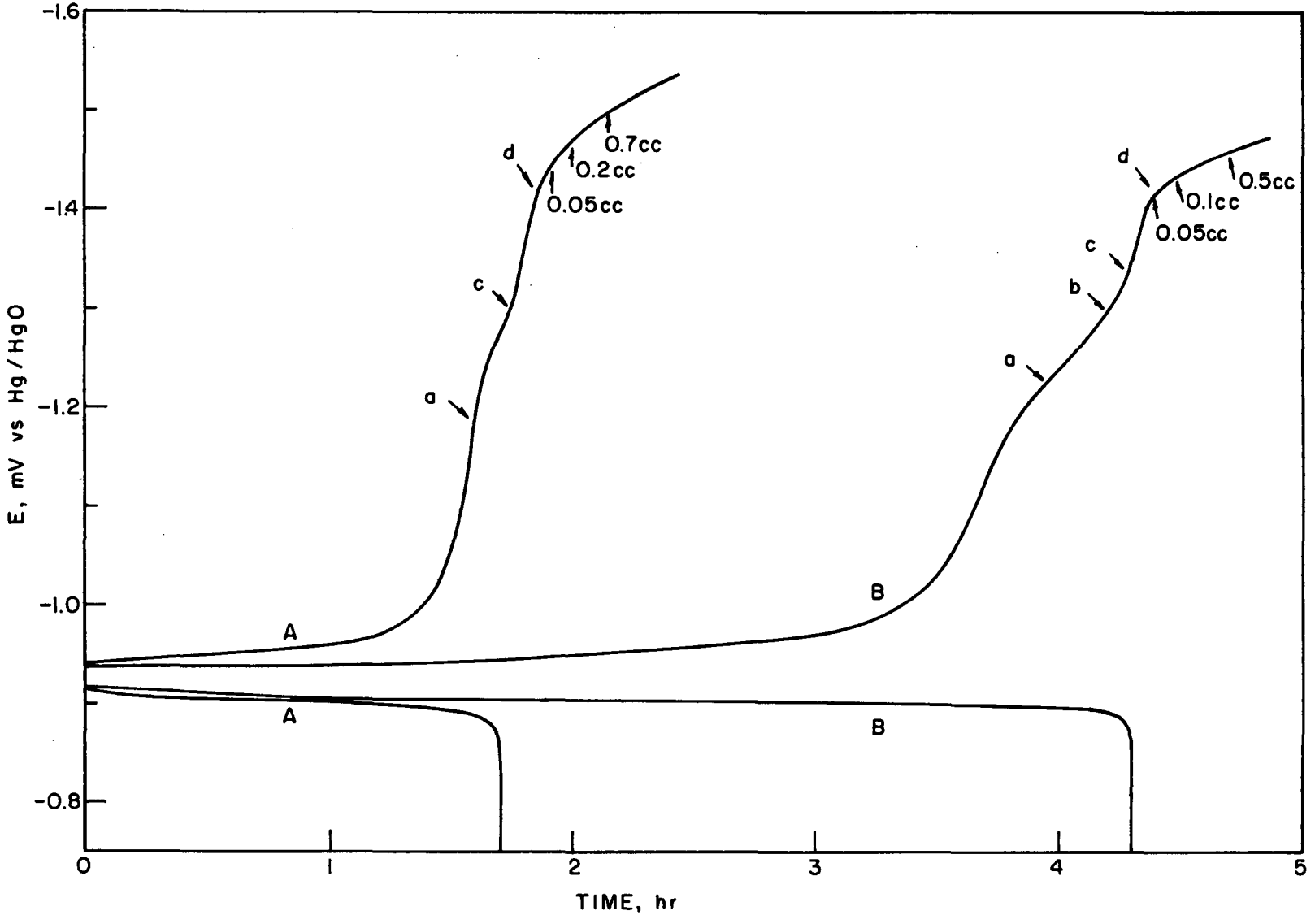

Fig. 5. Charge and discharge cycles of Teflon-bonded Cd electrode TFE-1 (25 °C, A = 14th cycle 5.5 mA/cm^2, B = 16th cycle 2.75 mA/cm^2; a = individual small bubbles, b = regularly small bubbles, c = slow gassing, d = moderate gassing)

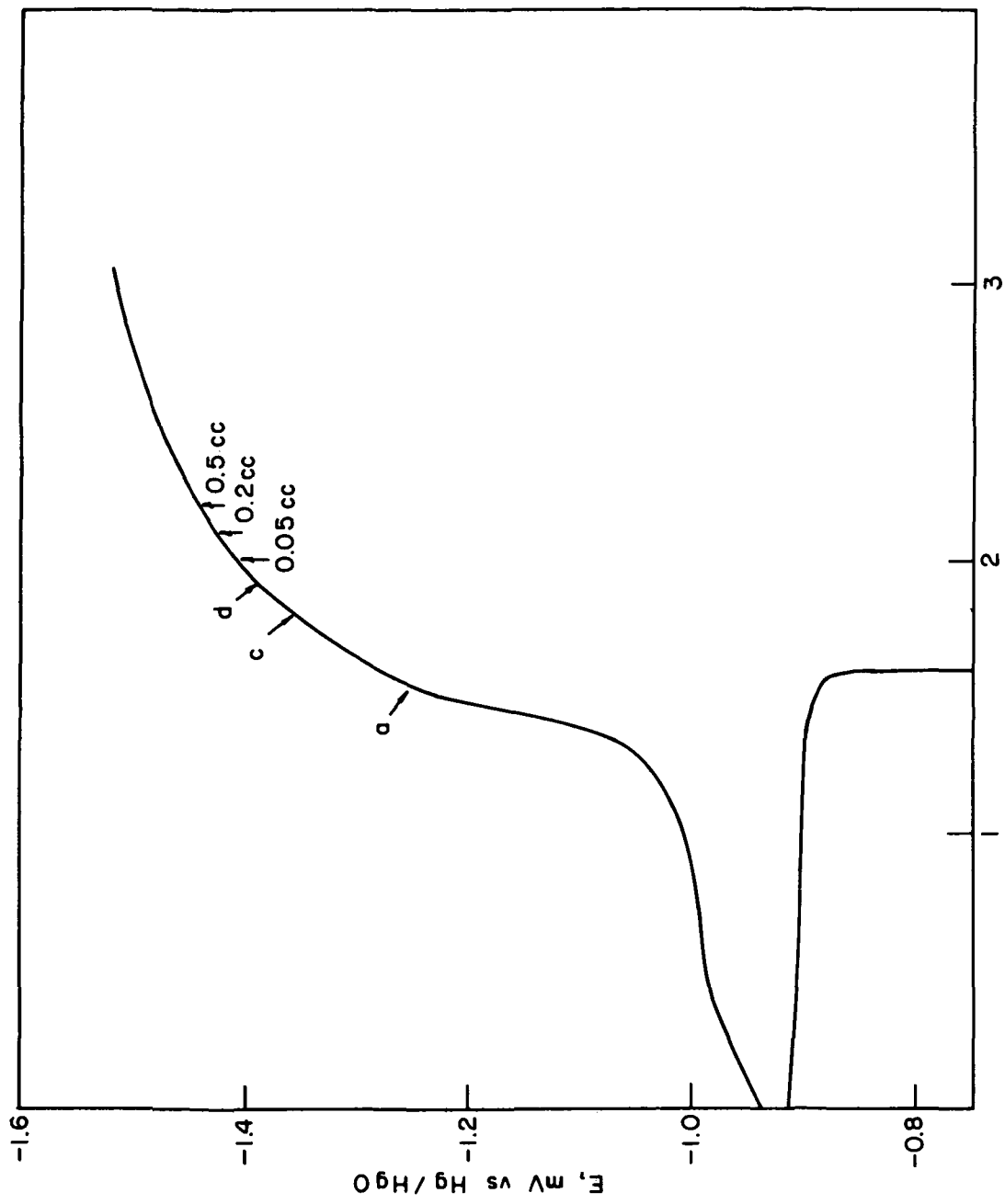

Fig. 6. Charge and discharge cycles of Teflon-bonded Cd electrode TFE-2 (15th cycle 25 °C, 7.4 mA/cm^2, a = individual bubbles, c = slow gassing, d = moderate gassing)

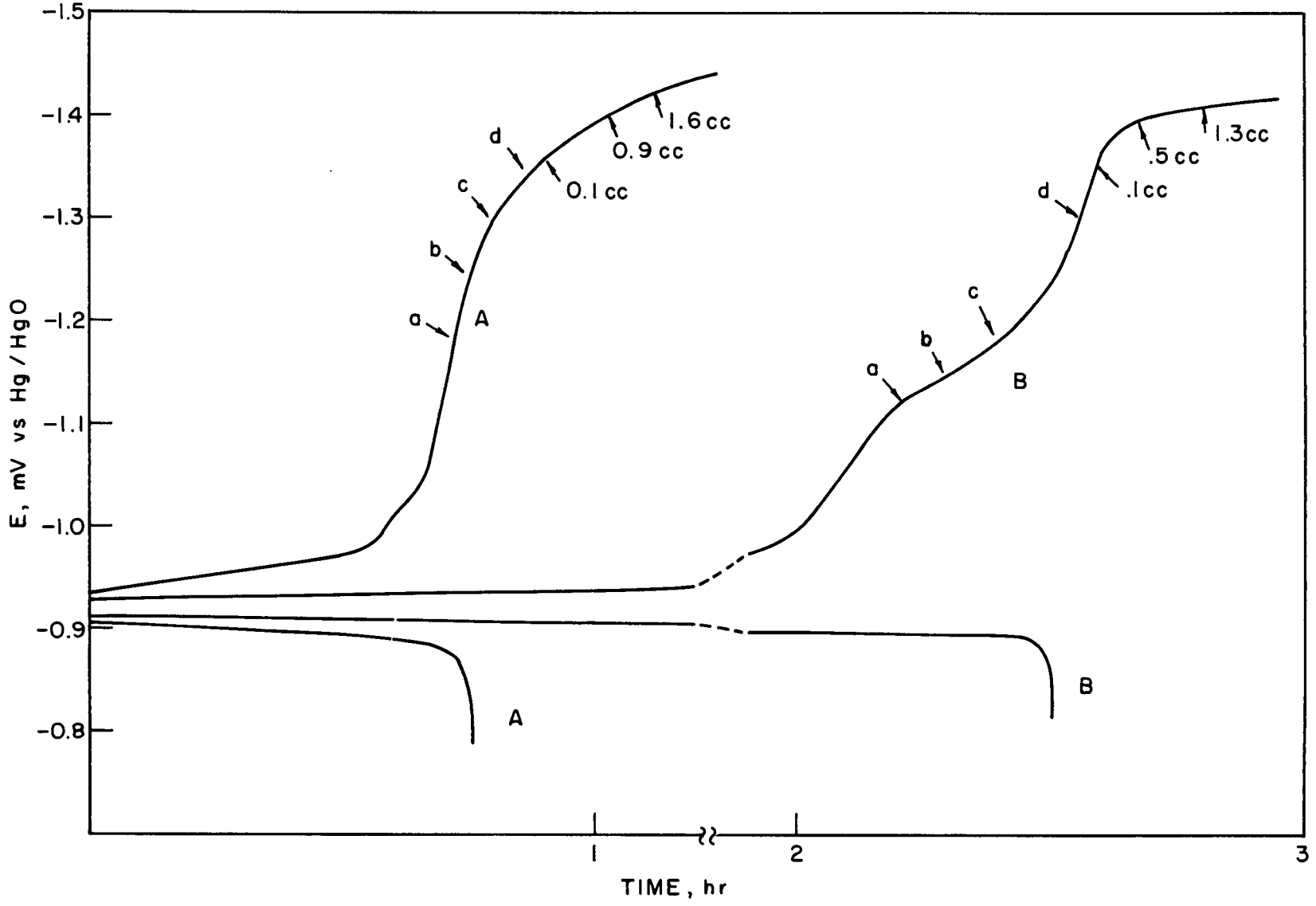

Fig. 7. Charge and discharge cycles of Teflon-bonded Cd electrode TFE-3 (A = 17th cycle, 8.3 mA/cm^2; B = 18th cycle, 4.15 mA/cm^2; a = first individual small bubbles; b = regularly small bubbles; c = weak gassing; d = moderate rate gassing)

The measured capacities of the Teflon-bonded cadmium electrodes given as a percentage of the theoretical capacity (calculated from the weight of the original electrode) are given in Table I as a function of cycle numbers. All electrodes showed a pronounced decrease in capacity with cycling. It is interesting to note that the good physical stability of electrode TFE-3 cannot be correlated to better retention of capacity. The more loosely packed electrode TFE-1 exhibits a lower initial capacity. However, after approximately 10 cycles, the differences between the three electrodes are not significant. In all cases, it was observed that extending the charge cycle into the hydrogen evolution region increased the capacity not only for the next discharge but for all following cycles. The 14th and 16th cycle of electrode TFE-1 and the change between cycles 16 and 22 of electrode TFE-3 demonstrate this effect. The discharge potentials and shape of the discharge curves are practically identical for all electrodes and independent of discharge rate.

Table I. Actual Capacity of Teflon-Bonded Cd-Electrodes as Fraction of the Theoretical Capacity (Charge and Discharge Rates Between C and C/2)

Number of Full Cycles	Electrode TFE-1	Electrode TFE-2	Electrode TFE-3
2	39	63	63
8	33	48	37
14	29	–	–
15	–	33	–
16	37.5	–	21
22	28	–	28
36	–	–	18

When judging the performance of these electrodes, it should be kept in mind that these data are exploratory in nature and that such parameters as the rate of charge and discharge varied with time and from electrode to electrode. Also the C and C/2 charge rate is fairly high when compared to conventionally used rates especially towards the end of the charging cycle.

2. Silver sinter-based cadmium electrodes (SSCd)

a. Electrode manufacture: A number of different silver powders and preparation techniques were used in exploring the fabrication of silver plaques with porosities about 70%. Table II lists the powders studied and their pertinent characteristics.

Table II. Selected Silver Powders and Some Pertinent Data*
(Supplier: Handy and Harman)

Minimum % Ag	99.6	99.9	99.99
Apparent density, $g/in.^3$	10 - 20	25 - 40	25.0
Fischer-sub-sieve sizer, μ	0.6 - 3.0	5 - 25	5.25
Screen analysis			
+ 100	–	0.5% max	–
+ 200	–	–	–
- 325	–	30.0% max	98.0%

*As supplied by the manufacturer's data sheet.

Our initial experiments were carried out at a sample of Silpowder 150. The Fischer average particle diameter was determined to be 10.4μ. Exploratory sintering runs were carried out at various temperatures and various times. A 28.4 mil mechanically sound plaque incorporating an expanded silver substrate (Exmet 5 Ag 7, 4/0) in the center of the porous mass was obtained by sintering at 600 °C for 30 min. The apparent porosity of the plaque was determined to be 75%. This corresponds to a powder porosity of 86%.

Encouraged by this result a larger batch of Silpowder 150 was ordered. The material obtained was determined to have a Fischer average particle diameter of 15.2 μ and an apparent bulk density of 2.52 g/cm^3 (tapped density 3.15 g/cm^3). Plaques fabricated in the same manner as the one described above had a porosity of 68.3%, corresponding to a powder porosity of 72.5%. This difference in porosity using the two different powders was reproducible. If the sintering temperature was

lowered to 550°C for 30 min, the porosity of plaques using Silpowder 150 could be increased to 70% corresponding to a powder porosity of 73.7%. Microsections of dry sintered plaques using the two kinds of Silpowder 150 are shown in Figs. 8 and 9. One can observe a very wide range of particle sizes and irregularly shaped agglomerates which form a network of large and small pores.

We also carried out sintering experiments on Silpowders 130 and 220. Silpowder 130 tended to form agglomerates and had poor flow characteristics which made accurate and reproducible plaque preparation difficult. We have, however, manufactured plaques of Silpowder 130 by sintering at 550°C for 30 min. These plaques have good mechanical strength and porosities of 76% (corresponding to a powder porosity of 82.5%). Silpowder 220 handled very well and resulted (under the same conditions described above) in plaques with 77% porosity (82% powder porosity). A more detailed investigation of these powders for plaque manufacture is in progress.

In addition to the dry sintering process, we also pursued a different approach which consisted of making a compact with an inert filler which is then leached out after sintering. Sodium fluoride was chosen as the filler. The silver powder and the NaF (60% by volume of solid NaF) were extensively mixed by rolling for 72 hr. The blended material was evenly distributed into a mold and compacted at 25,000 psi. The resulting compact was then sintered at 600°C for 30 min followed by leaching in water. Using Silpowder 220, a sound mechanical structure was obtained with an apparent porosity of 70% (powder porosity of 75%). A microsection of this structure is shown in Fig. 10. The particle size of this powder is smaller and much more uniform than that of Silpowder 150 which results in a much more uniform pore size distribution.

For comparison purposes, Fig. 11 shows a microsection of a typical dry sintered nickel plaque of carbonyl nickel (Type 287) sintered at 900°C for 40 min in a hydrogen atmosphere. The apparent particle size of the carbonyl nickel is considerably smaller than that of the silver powders and quite uniform. The structure shows also a dual porosity (large and very small pores).

Dry silver sinters, especially of Silpowder 220, are presently under closer investigation. We are also exploring whether higher porosities (80% or more) can be obtained by increasing the amount of NaF filler without compromising the mechanical strength of the resulting plaques. At comparable apparent porosities, there appears

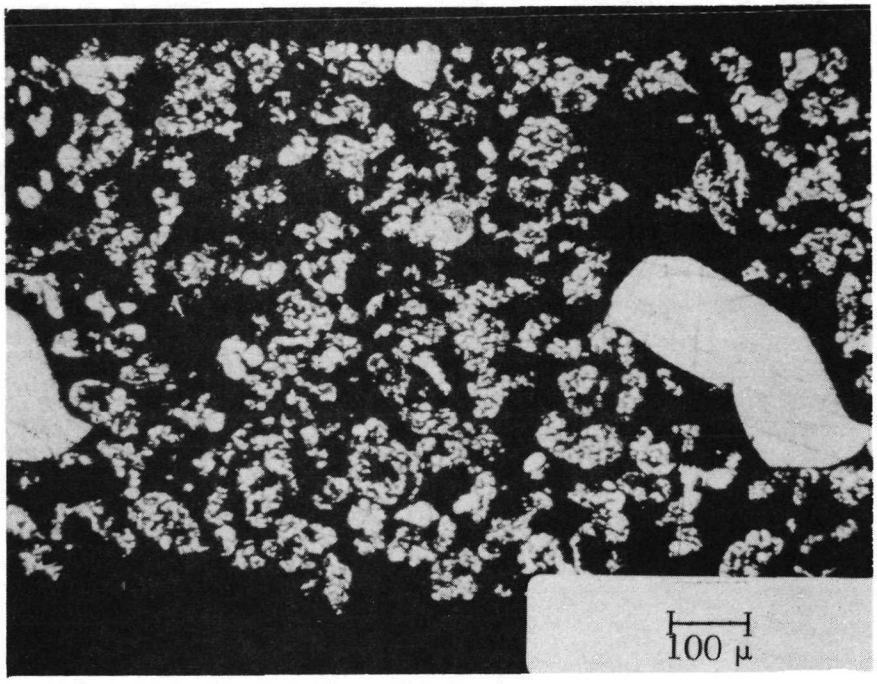

Fig. 8. Ag sinter plaque (Silpowder 150, FAPD 10.4 μ, dry layup)

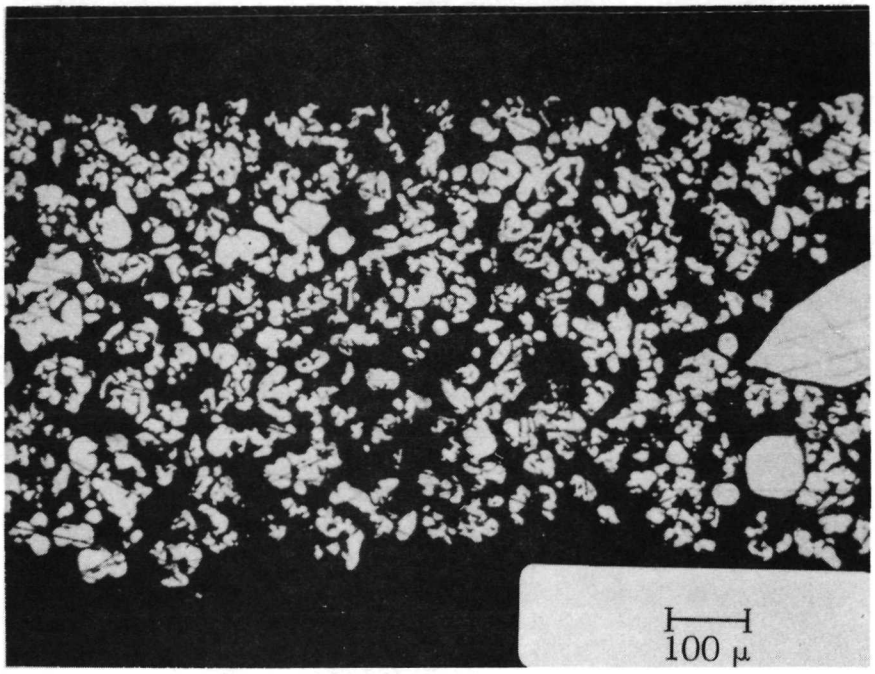

Fig. 9. Ag sinter plaque (Silpowder 150, FAPD 15.2 μ, dry layup)

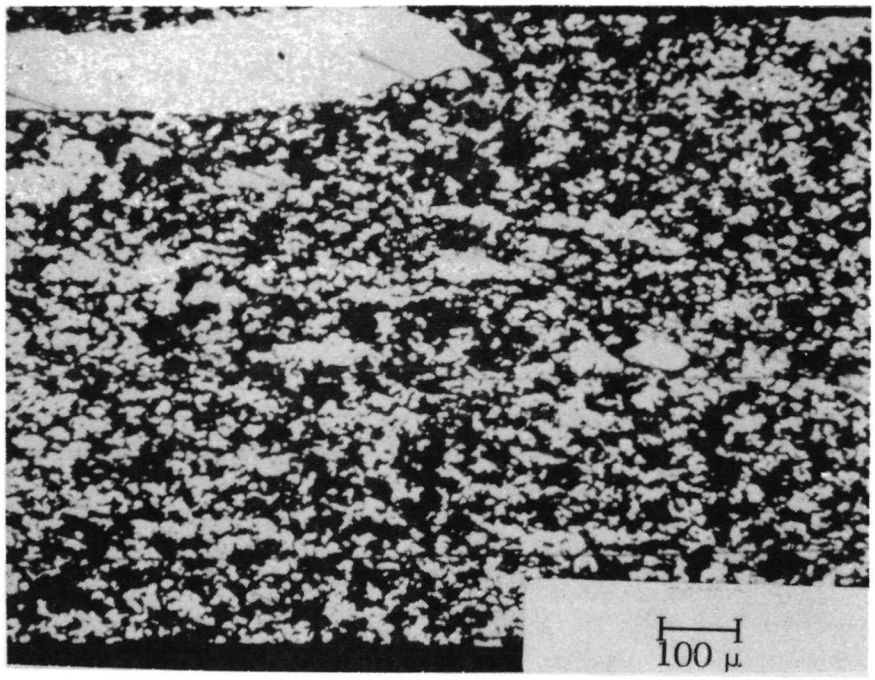

Fig. 10. Ag sinter plaque (Silpowder 220, NaF compact)

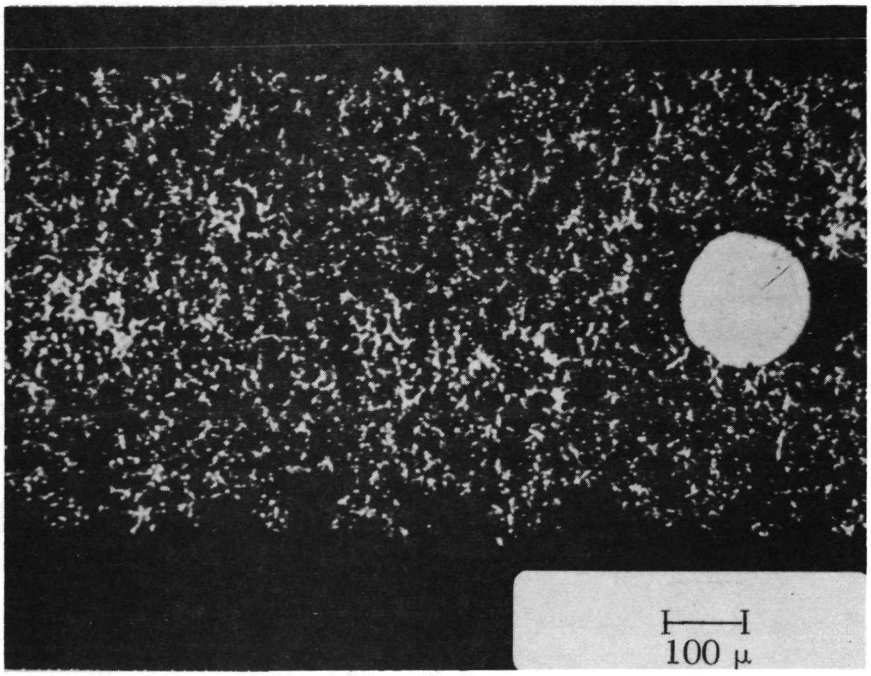

Fig. 11. Ni plaque (Carbonyl Ni type 287, dry layup)

to be significant differences in the structure of pressed and loosely sintered plaques which may influence the electrochemical performance of impregnated plates.

b. Electrochemical evaluation: The silver sinter Cd electrode SSCd-1 was obtained by four chemical impregnations (Saft process) of a porous silver plaque obtained by sintering a dry layup of Silpowder 150 (600°C for 30 min, porosity 75%). The theoretical capacity of the 1- × 1.5-in. electrode was 0.364 Ahr. The electrode was cycled between -1.2 V and -0.8 V versus Hg/HgO at current densities corresponding to rates between C and C/2. Typical potential-time curves during cycling are shown in Figs. 12 and 13. The potential-time curves during charge are characterized by a flat plateau followed by a sharp rapid potential change at the end of charge. The first individual gas bubbles were observed at -1.24 V versus Hg/HgO. Also, the transition to the limiting charge potential determined by hydrogen evolution is much sharper than observed at the Teflon-bonded electrodes earlier. A comparison of the shape of the potential-time curves of the Teflon-bonded electrodes and the impregnated Ag plaque demonstrate clearly the effect of electrode structure. It also confirms our interpretation of the gradual potential decrease at Teflon-bonded electrodes as being caused mainly by poor electronic contact throughout the electrode structure. The capacity changes of this electrode as a function of cycle number are shown in Table III. Some shedding of surface $Cd(OH)_2$ was observed during cycling. The rate of capacity loss during cycling was somewhat reduced in comparison to the Teflon-bonded electrodes. This relatively large change in capacity during cycling could be a consequence of the specific electrode structures or of the testing conditions employed. This effect will require further investigation.

Table III. Capacity of Silver Sinter Based Cd Electrode SSCd-1 as Fraction of Theoretical Capacity.

Number of Cycles	Capacity (% of Theoretical Capacity)
2	51.5
20	43.4
41	25.4
60	12.2
94	6.6

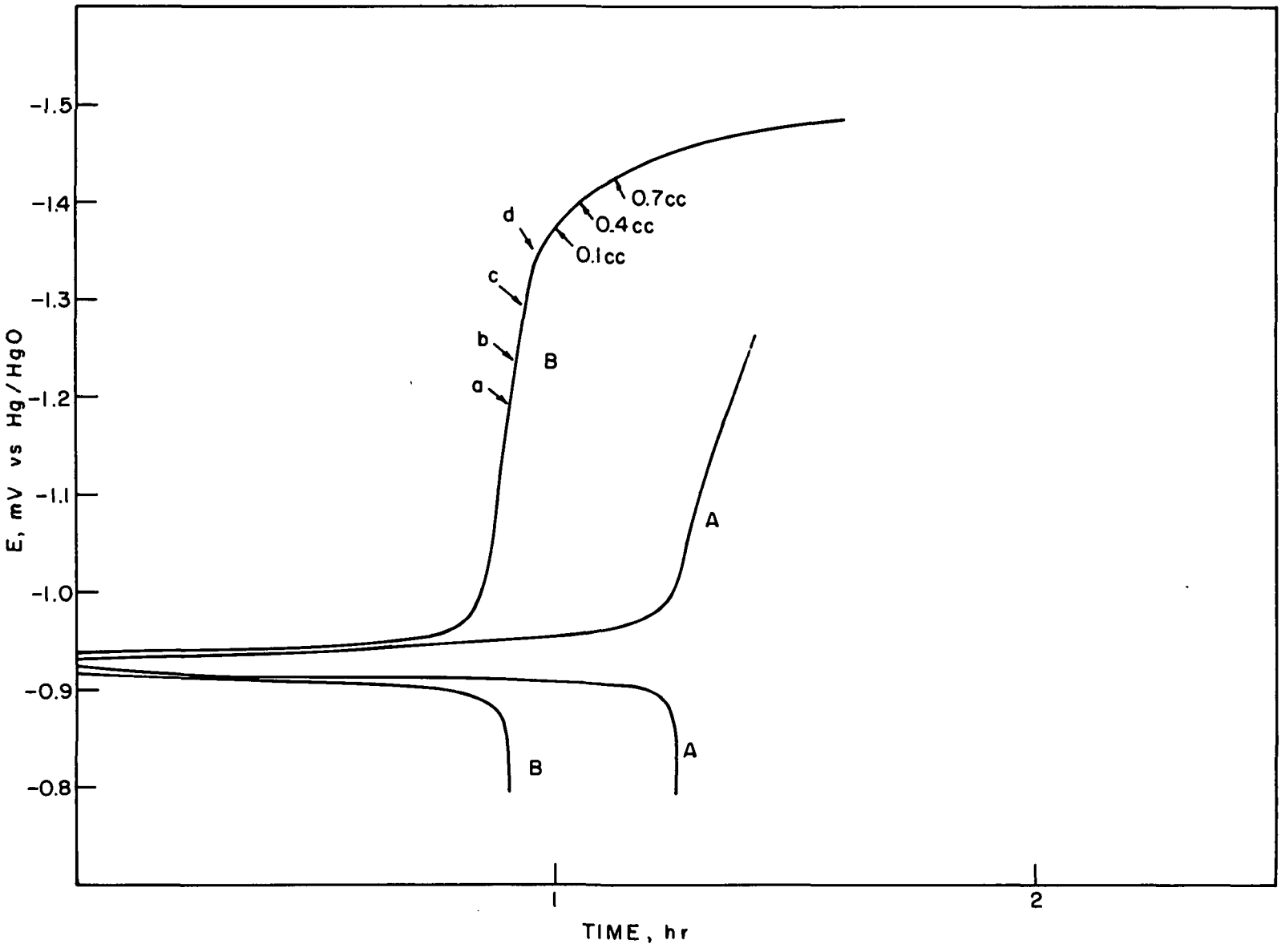

Fig. 12. Ag sinter Cd electrode, SSCd-1 (A = 2nd cycle, 15.5 mA/cm^2; B = 5th cycle, 15.5 mA/cm^2; a = first small individual bubbles; b = regularly small bubbles; c = weak gassing; d = moderate gassing)

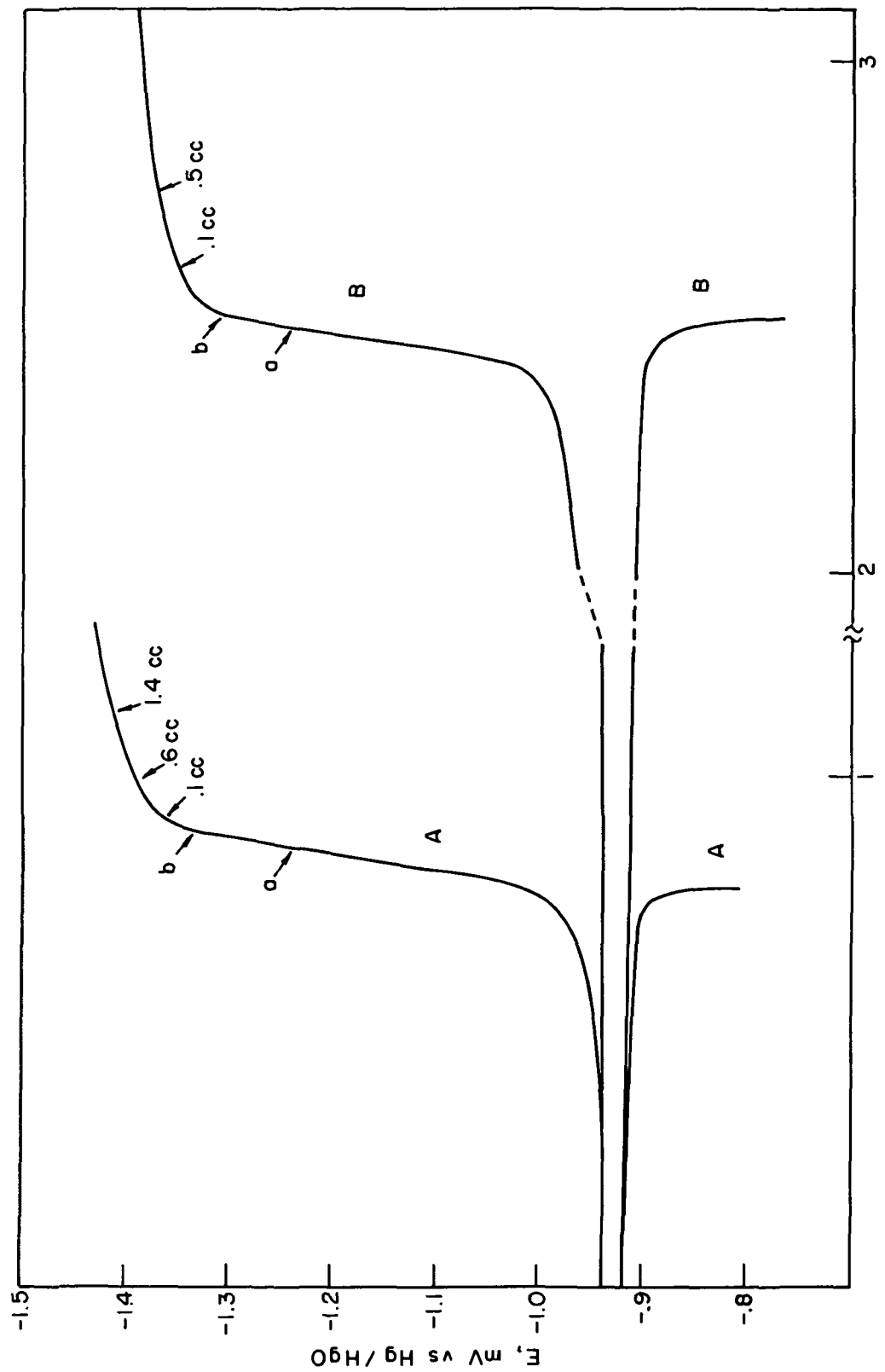

Fig. 13. Ag sinter Cd electrode, SSCd-1 (A = 40th cycle, i = 7.75 mA/cm^2; B = 43rd cycle, i = 3.1 mA/cm^2; a = first bubbles at active top center of electrode; b = first bubbles all over electrode)

3. Nickel Sinter-Based Cadmium Electrodes (NSCd)

For comparison purposes, we also cycled a conventional Cd electrode on a sintered nickel substrate (NSCd-1). Strong hydrogen evolution was observed at -1.075 V versus Hg/HgO on charging at 100 mA (C/4 rate). The potentiostatic current-voltage curve for this electrode is shown in Fig. 14.

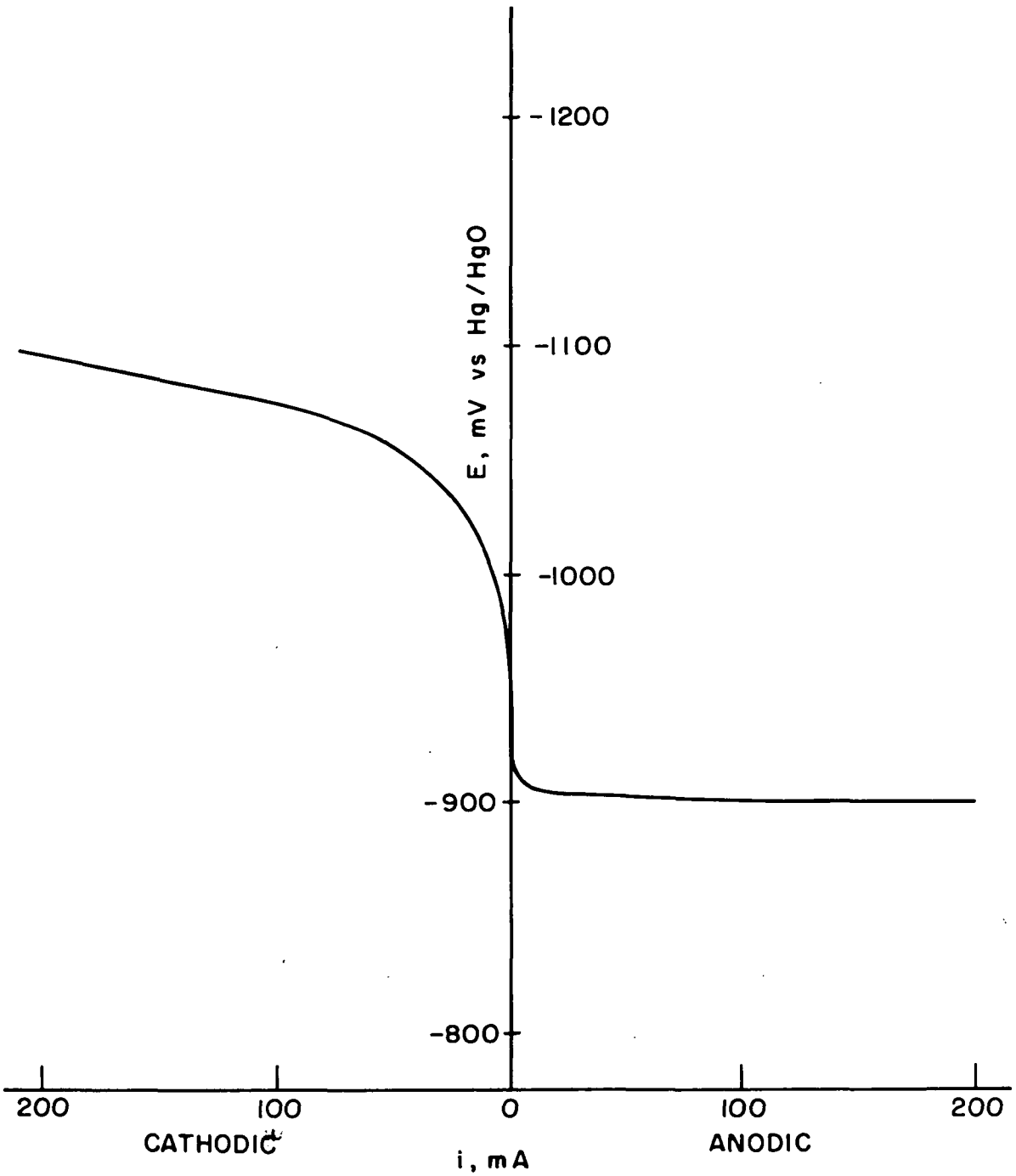

Fig. 14. Potentiostatic current voltage curve at a Cd electrode of a conventional GE aerospace cell NSCd-1 (25% KOH, 25 °C, 200 mA = C/2 rate)

III. FUTURE WORK

We will continue to explore fabrication techniques and examine the electrochemical behavior of the various plaque structures proposed for negative plates. On the basis of this investigation, we will then fabricate 24 Cd electrodes with three different loadings for each of the five different current collector materials. These electrodes will be subjected to an extended electrochemical test program in which the voltage, capacity, and the "point of advent" of gas evolution will be measured as function of charge rate and temperature. In addition, 24 nickel electrodes with three different loadings will be fabricated and tested for the amount of O_2 evolution as a function of capacity. For this testing program, an automatic battery cycler is under construction. This unit will permit cycling of electrodes between either preset voltages or the onset of gas evolution.

IV. REFERENCES

1. E.J. Rubin and R. Baborian, J. Electrochem. Soc., 118, 428 (1971).
2. D. MacArthur, J. Electrochem. Soc., 117, 422 (1970).
3. O. Glemser and J. Einerhand, Z. Elektrochem., 54, 302 (1950).
4. E.J. McHenry, Electrochem. Tech., 5, 275 (1967).
5. P.U. Popat and E.J. Rubin, Final Report JPL Contract No. 951972.
6. F.G. Will, NASA/GSFC Battery Workshop, November 1970.
7. T.S. Lee, J. Electrochem. Soc., 118, 1278 (1971).